

Some recent advances on superfast 3D shape measurement with digital binary defocusing techniques



Beiwen Li^a, Yajun Wang^a, Junfei Dai^b, William Lohry^a, Song Zhang^{a,*}

^a Mechanical Engineering Department, Iowa State University, Ames, IA 50011, United States

^b Mathematics Department, Zhejiang University, Zhejiang 310027, China

ARTICLE INFO

Article history:

Received 18 April 2013

Received in revised form

3 July 2013

Accepted 10 July 2013

Available online 3 August 2013

Keywords:

Binary defocusing

Digital fringe projection

3D shape measurement

Dithering

Pulse width modulation

ABSTRACT

The digital binary phase-shifting technique has been demonstrated for its merits over the conventional sinusoidal phase-shifting method in terms of measurement speed and simplicity. Yet, the measurement depth range is small when a squared binary method is used. Our recent research focuses on improving its measurement accuracy without sacrificing measurement speed, and increasing its depth range without losing measurement quality. This paper will summarize our recent work on the following three major areas: (a) realization of kHz 3D shape measurement with binary phase-shifting methods; (b) binary pattern improvement with pulse width modulation and binary dithering/halftoning techniques; and (c) applications of superfast 3D shape measurement techniques. Principle of each technique will be presented, and experimental results will be shown to verify its performance.

© 2013 Elsevier Ltd. All rights reserved.

1. Introduction

Digital fringe projection (DFP) techniques have been extensively used for high-quality 3D shape measurement due to their speed, accuracy, and flexibility [1,2]. A conventional DFP system utilizes a computer to generate sinusoidal fringe patterns that are projected by a projector, a camera to capture the scattered patterns by the object surface, and finally a fringe analysis software to retrieve the phase for three-dimensional (3D) shape reconstruction. Since a typical sinusoidal fringe pattern requires 8 bits, the measurement speed is limited by the maximum frame rate of the projector (typically 120 Hz) [3]. Furthermore, most of the video projectors are nonlinear, making it difficult to generate high quality phase without nonlinearity calibration and correction [4]. Though numerous nonlinear calibration techniques [5–10] have been developed and demonstrated their successes, we found that the problem is more complex than it seems to be since the projector's nonlinear gamma actually changes over time.

To overcome the limitations of the conventional DFP techniques, we proposed the squared binary defocusing technique [11]. Instead of utilizing 8-bit grayscale patterns, the binary defocusing technique only requires 1-bit binary structured patterns, and sinusoidal fringe patterns are naturally blended together by positioning the object away from the focal plane of the projector.

This technique is not affected by the nonlinearity of the projector since only two intensity values are used. Moreover, since only 1-bit structured patterns are required, the binary defocusing technique drastically reduces the data transferring rate, making it possible to achieve faster than 120 Hz 3D shape measurement speed. Taking advantage of the digital-light-processing (DLP) Discover platform, we have successfully developed a system that could achieve tens of kilo-Hertz (kHz) 3D shape measurement speed [12]. However, the binary defocusing technique is not trouble free. The measurement capability is rather limited comparing with a conventional DFP method: (a) the measurement accuracy is lower due to the influence of high-frequency harmonics; (b) the depth measurement range is smaller since the object must be properly placed in a small region such that the binary pattern becomes good-quality sinusoidal [13]; (c) the calibration is more involved because most of the existing calibration techniques require the projector to be in focus [14]; and (d) it is difficult to simultaneously achieve high-quality fringe patterns for different spatial frequencies [15].

A number of methods have been developed to address the limitations of the binary defocusing techniques. Our research [16] found that increasing the number of phase-shifted fringe patterns could reduce the error caused by high-frequency harmonics if a least-squares (LSQ) fringe analysis method is adopted. Moreover, since a squared wave only has odd-number harmonics without even ones, using an odd-number phase-shifting algorithm is preferable for a DFP system where the phase shift errors can be completely eliminated. Furthermore, compared with sinusoidal

* Corresponding author. Tel.: +1 515 294 0723; fax: +1 515 294 3261.
E-mail address: song@iastate.edu (S. Zhang).

fringe patterns, the binary pattern has better fringe contrast, and thus has the potential to better measure microstructure [17]. However, the enhanced measurement quality was achieved by utilizing more fringe patterns, which usually means sacrificing measurement speed. For high-speed applications, this approach is not desirable.

To enhance the binary defocusing method without increasing the number of required structured patterns, modulating the squared binary patterns is probably the only option since for a conventional DFP technique, the sinusoidal fringe patterns only vary in one direction. Improving squared binary patterns becomes optimizing the square wave such that it is easier to generate sinusoidal fringe patterns through low-pass filtering. It turns out that significant efforts have been made in the Power Electronics field to realize better sinusoidal wave using binary levels through pulse width modulation (PWM) techniques. This idea has been borrowed to the 3D shape measurement field. Fujita et al. [18] and Yoshizawa and Fujita [19] implemented the PWM technique through hardware, and Ayubi et al. [20] has introduced the sinusoidal pulse width modulation (SPWM) technique to shift non-fundamental frequency to higher frequency components such that they can be easier to be suppressed by defocusing; and the improvement was noticeable for a certain range of fringe breadths. Wang and Zhang [21] have developed the optimal pulse width modulation (OPWM) technique to further improve phase quality. By taking advantage of the phase-shifting algorithm and selectively reducing the high-frequency harmonics influences, the OPWM technique and its variation [22] could drastically improve the fringe quality, and even good quality sinusoids of different fringe frequencies could be simultaneously obtained such that a multifrequency phase-shifting algorithm can be realized [15]. However, the improvement of OPWM or SPWM technique is still limited if the fringe stripes are too narrow or too wide [23].

Due to the discrete nature of the fringe patterns, it is understandable that the PWM techniques have limited improvements. This is because, the PWM techniques are, after all, one dimensional in nature. Therefore, there are large room for further improvement if the optimization can be performed in both dimensions. Xian and Su proposed an interesting area modulation technique that utilized highly precisely micro-machined gratings [24]. This technique could generate high-quality sinusoidal fringe patterns if the manufacturing precision is high enough, and the dots are small enough (in micron-meters). However, this technique cannot be easily adopted to a DFP system since the pixel size is much larger than the required dot size. We recently proposed a technique to locally modulate the pixels to emulate a triangular pattern to reduce high-frequency harmonics influences [25]. This technology is advantageous as it permits the use of nearly focused patterns, and the improvement is significant if the fringe stripe is narrow. However, similar to PWM techniques, this area-modulation technique has limited improvement when fringe stripes are wide.

We recently noticed that representing grayscale images with binary images has been extensively studied in the digital image processing field for high-quality printing. This technology is called half-toning or dithering, which has been originated since the 1960's [26]. Over the years, researchers have come out with a number of dithering techniques [27–31]. Among these techniques, the ordered-Bayer dithering technique and the variations of error-diffusion techniques have been extensively used. We have borrowed the simple Bayer-dithering technique [32] and later the error-diffusion techniques to the 3D shape measurement field [33]. Our research found that the dithering techniques drastically improve the measurement quality when the fringe stripes are wide, yet the improvement is limited if the fringe stripes are narrow.

The majority of the dithering techniques are simply applying a matrix to the grayscale images, and binarize the image by

comparing the original or modified intensity with the matrix. These algorithms were all developed to generate best quality visual effect for generic grayscale images. Yet, they were not specifically designed to take advantages of some inherent structures of the grayscale images, e.g., sinusoidal structures for fringe patterns. Therefore, great improvements could be achieved if we utilize the inherent unique sinusoidal structures of the fringe patterns. Lately, we have developed a couple of algorithms [34,35] to optimize the dithering techniques, and substantial improvements have been achieved.

This paper summarizes our recent work on superfast 3D shape measurement with the binary defocusing techniques. Specifically, we will summarize the following three major accomplishments: (a) realization of kHz 3D shape measurement with binary phase-shifting methods; (b) binary pattern improvements with PWM and binary dithering/halftoning techniques; and (c) applications of superfast 3D shape measurement techniques. The principles of each technique will be presented, and some experimental data will be shown.

Section 2 explains the principle of these techniques. Section 3 shows some experimental results, and finally Section 4 summarizes this paper.

2. Principle

2.1. Fundamentals of binary defocusing techniques

A binary pattern can be regarded as a square wave in mathematics. If we take Fourier series expansion of the square wave, the first order harmonic represents the ideal sinusoidal wave, while higher order harmonics represent the detailed features of the square wave. It is worth to note that the square wave only contains odd-order harmonics, which indicates that if a low pass filter that can eliminate or suppress higher order harmonics is applied, ideal sinusoidal wave can be approximated. Projector defocusing technique could create smoothing effect towards the image which can be modelled as a Gaussian filter, which means that if the projector is properly defocused to a certain degree, the projected binary image would be blurred such that a quasi-sinusoidal fringe pattern can be generated [11].

Fig. 1(a and b) shows the example of a squared binary pattern and its resultant pattern after Gaussian smoothing. Here, a Gaussian filter with the size of 13×13 and standard deviation of $13/3$ is used in order to emulate the projector defocusing effect. Fig. 1(c and d) shows their corresponding cross sections. This simulation indicates that if the projector is properly defocused, a quasi-sinusoidal fringe pattern can be very well represented.

2.2. Three-step phase-shifting algorithm

Phase-shifting algorithms have been extensively adopted in high-quality 3D shape measurement; and a number of phase-shifting algorithms have been developed. In this research, a simple three-step phase-shifting algorithm with a phase shift of $2\pi/3$ was used to test the generated pattern. Three fringe images can be described as

$$I_1(x, y) = I'(x, y) + I''(x, y) \cos[\phi - 2\pi/3], \quad (1)$$

$$I_2(x, y) = I'(x, y) + I''(x, y) \cos[\phi], \quad (2)$$

$$I_3(x, y) = I'(x, y) + I''(x, y) \cos[\phi + 2\pi/3] \quad (3)$$

where $I'(x, y)$ is the average intensity, $I''(x, y)$ the intensity modulation, and $\phi(x, y)$ the phase to be solved for

$$\phi(x, y) = \tan^{-1} \frac{\sqrt{3}(I_1 - I_3)}{2I_2 - I_1 - I_3}. \quad (4)$$

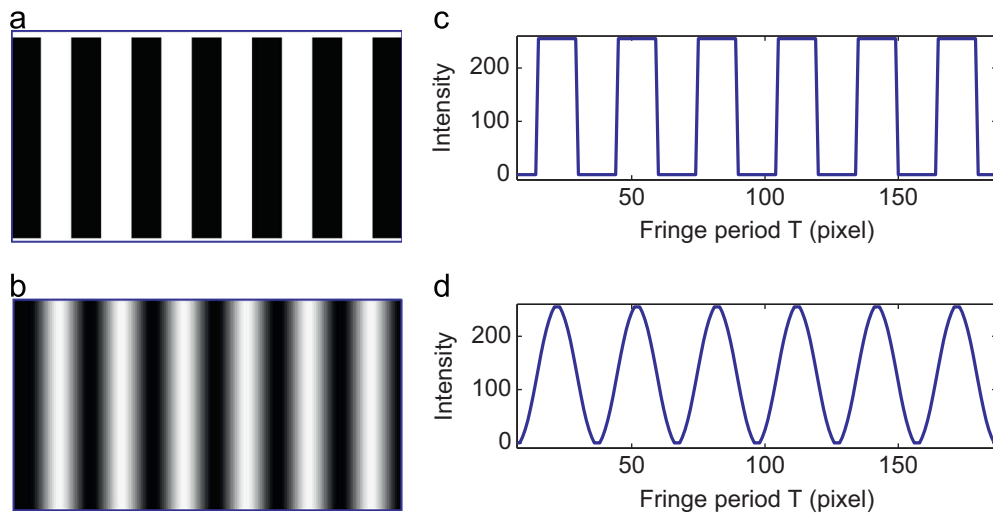


Fig. 1. Example of applying a Gaussian filter to a squared binary pattern can result in a quasi-sinusoidal pattern. (a) A squared binary pattern with a period $T=30$ pixels. (b) The resultant pattern of (a) after Gaussian smoothing with filter-size of 13×13 . (c) Cross section of (a). (d) Cross section of (b).

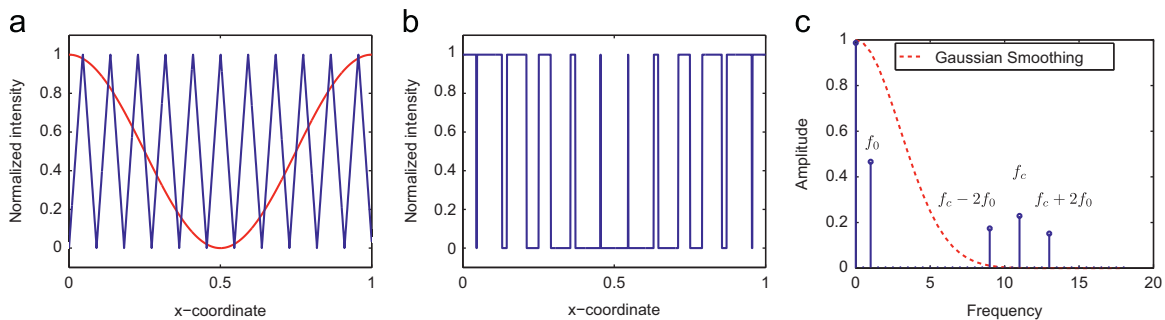


Fig. 2. (a) Sinusoidal wave and triangular wave with $f_c = 11f_0$. (b) Resultant PWM pattern. (c) FFT and Gaussian smoothing curve [20].

This equation provides the phase range $[-\pi, +\pi)$ with 2π discontinuities. A continuous phase map can be obtained by adopting a spatial or temporal phase unwrapping algorithm. In this research, we used the temporal phase unwrapping framework introduced in [36].

2.3. Superfast phase shifting with binary defocusing technique

Traditionally, a digital fringe projection technique with a phase-shifting method requires sinusoidal fringe patterns that contain 8-bit images, and thus, the speed of measurement is usually limited to 120 Hz due to the limit of the image switching rate of a digital video projector. Recently, the rapid development of DLP technology has enabled to switch 1-bit binary images at a rate of tens of kHz, which means that by using a binary defocusing technique plus a three-step phase-shifting algorithm, the speed of measurement can be theoretically extended to the magnitude of kHz. Zhang et al. [12] has successfully developed a system with a fringe acquisition rate of 2000 Hz. In other words, the speed of 3D shape measurement can be extended up to 667 Hz since a three-step phase-shifting algorithm was used. In addition to the great speed improvement, the system also has the advantage of (1) no precise synchronization between the projector and the camera; (2) no projector nonlinear gamma correction necessary; and (3) high spatial and temporal resolution [12]. Such a technique has been successfully used to measure extremely rapidly changing scene, such as rabbit hearts [33]. Yet, as previously addressed, the squared binary defocusing technique has limited measurement depth range.

2.4. Pulse width modulation techniques

In order to better represent sinusoidal wave with binary defocusing technique, attempts were first made to modulate the binary patterns in 1-D, which includes sinusoidal pulse width modulation (SPWM) technique introduced by Ayubi et al. [20] and optimal pulse width modulation (OPWM) technique introduced by Wang and Zhang [21].

The main objective of SPWM technique is to shift the undesired order of harmonics to higher frequency such that the performance of binary defocusing technique would be enhanced with a smaller degree of defocusing. Fig. 2(a) illustrates the basic principle of SPWM technique. Here, the desired sinusoidal wave with frequency f_0 is compared to a triangular wave with a higher frequency f_c . The grayscale value of the SPWM pattern will be set to 1 if the intensity of sinusoidal wave is higher than that of triangular wave, or will be set to 0 otherwise. Fig. 2(b) shows the resultant pattern and Fig. 2(c) shows the spectrum of the pattern after taking fast Fourier transform (FFT), from which it can be discovered that by choosing the frequency f_c , the undesired order of harmonics can be shifted away from the fundamental frequency in a controllable manner, which would facilitate binary defocusing technique with comparatively smaller degree of defocusing.

However, it has been discovered that SPWM only surpasses squared binary method within a certain number of fringe periods [21], then Wang and Zhang proposed an OPWM technique to overcome this challenge. Rather than shifting the undesired harmonics realized by SPWM technique, the OPWM technique selectively eliminates the undesired harmonics, which has been proved successful with a large range of fringe periods. Fig. 3 shows

a typical example of OPWM pattern. Due to its property of half-cycle symmetry, its Fourier coefficients are left only with odd-order harmonics b_k . b_k can be written as follows:

$$b_k = \frac{4}{\pi} \int_{\theta=0}^{\pi/2} f(\theta) \sin(k\theta) d\theta \quad (5)$$

Then, considering the Quarter-wave symmetric waveform as shown in Fig. 3, we have

$$b_k = \frac{4}{\pi} \int_0^{\alpha_1} \sin(k\theta) d\theta - \frac{4}{\pi} \int_{\alpha_1}^{\alpha_2} \sin(k\theta) d\theta + \frac{4}{\pi} \int_{\alpha_2}^{\alpha_3} \sin(k\theta) d\theta \dots - \frac{4}{\pi} \int_{\alpha_n}^{\pi/2} \sin(k\theta) d\theta. \quad (6)$$

Since we have n unknown values $(\alpha_1, \alpha_2 \dots \alpha_n)$, it is possible to eliminate $n-1$ selected order of harmonics and meanwhile keep the fundamental frequency with desired magnitude by simultaneously solving the equations ($b_1=m$, $b_{k_1}=0$, $b_{k_2}=0 \dots b_{k_{n-1}}=0$), here m refers to the desired magnitude.

Fig. 4(a) shows an example of SPWM pattern with the fringe period of $T=60$. Fig. 4(b) shows an example of OPWM pattern with the fringe period of $T=60$. Fig. 4(c) shows the simulation results of the comparison between squared binary method (SBM), OPWM and SPWM if different fringe periods are utilized. Here, a small Gaussian filter with the size of 5×5 and standard deviation of $5/3$ pixels is used to simulate the small amount of defocusing. The simulation results indicate that when the fringe period is very small $T=18$, SBM has the best performance. Also, SPWM technique is only superior to SBM technique when the fringe period is large,

while OPWM outperforms both SPWM and SBM in the majority cases [21].

2.5. Dithering techniques

In order to further improve the fringe quality, there are several techniques carried out to modulate the fringe patterns in 2-D. One of the most well-known techniques is binary dithering. Binary dithering refers to a technique that renders the original image with only two-bit color and meanwhile randomizes the quantization error [32]. Fig. 5 illustrates the example of dithering techniques on a general grayscale image, and then on a sinusoidal pattern. In this subsection, three most extensively used dithering techniques will be introduced, which include bayer-ordered dithering technique [28], Floyd–Steinberg error-diffusion dithering technique [30] and Stucki error-diffusion dithering technique [31].

The Bayer-ordered dithering technique, rather than using a simple threshold, compares the original image with a 2D grid of thresholds called Bayer kernel, and then the original image is quantized according to the corresponding pixels in the Bayer kernel. Typically the threshold values in the dither pattern are different from one to another, and thus the randomization of quantization error is achieved somehow. According to Bayer [28], an optimal dithered image with the noise being as high frequency as possible can be achieved if the size of the Bayer kernel is 2^N . Then the noise can be effectively reduced by a low-pass filter. The simplest Bayer dither pattern with a size of 2×2 can be obtained as follows:

$$M_1 = \begin{bmatrix} 0 & 2 \\ 3 & 1 \end{bmatrix}, \quad (7)$$

Then, larger Bayer kernel can be obtained by

$$M_{n+1} = \begin{bmatrix} 4M_n & 4M_n + 2U_n \\ 4M_n + 3U_n & 4M_n + U_n \end{bmatrix}, \quad (8)$$

where U_n refers to an $n \times n$ unit matrix. After applying the Bayer kernel, the original image is then effectively quantized according to the threshold values in the Bayer kernel. For the Binary defocusing technique, ideal sinusoidal patterns can be quantized by this Bayer-ordered dithering. It has been proved that Bayer-ordered

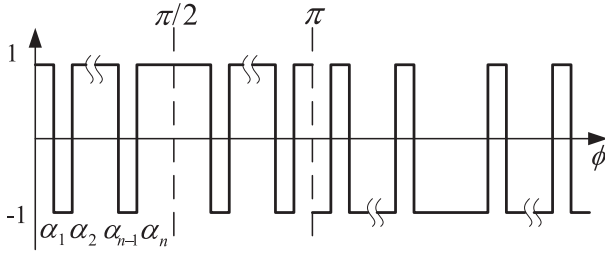


Fig. 3. Quarter-wave symmetric OPWM waveform [21].

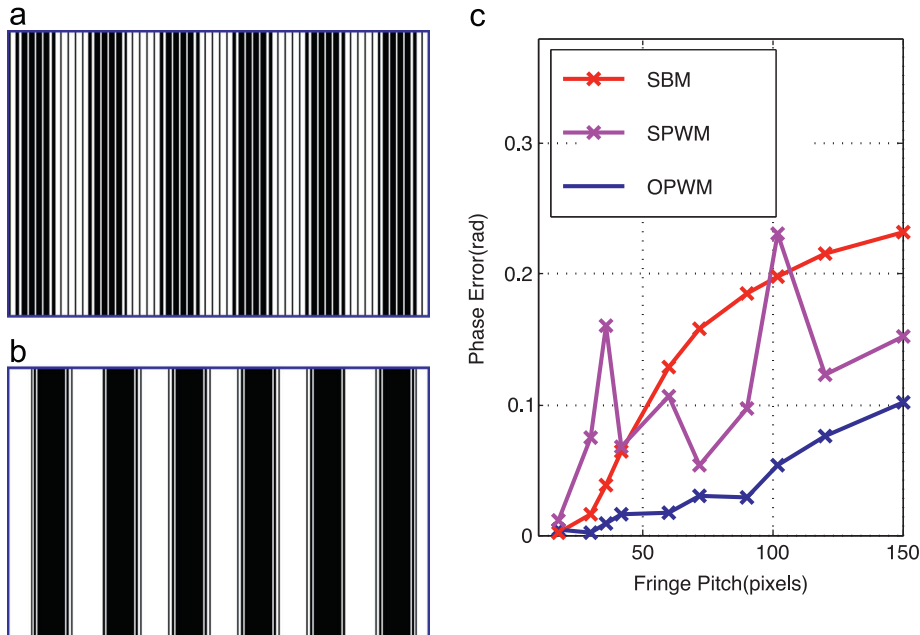


Fig. 4. (a) An SPWM pattern with $T=60$. (b) An OPWM pattern with $T=60$. (c) Simulation results of the SBM, SPWM and OPWM patterns with different fringe periods.

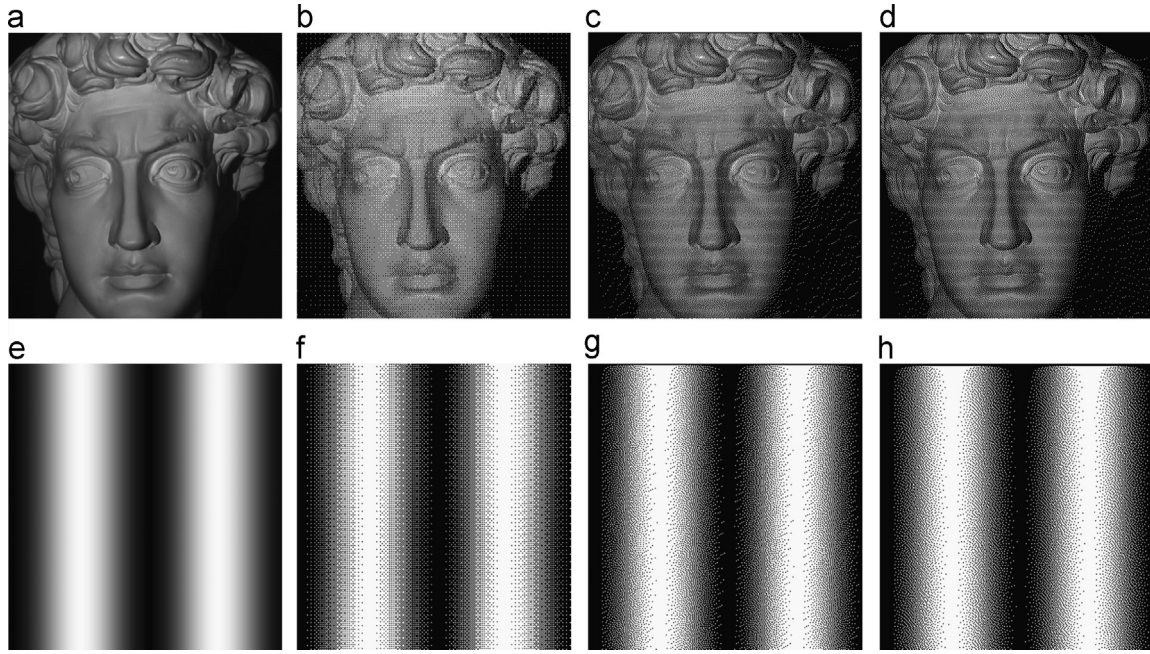


Fig. 5. (a) Original image of a general 8-bit grayscale image. (b) Binary dithered image of (a) using Bayer-ordered dithering technique. (c) Binary dithered image of (a) with the Floyd–Steinberg error-diffusion technique. (d) Binary dithered image of (a) with the Stucki error-diffusion technique. (e) Original image of a sinusoidal fringe pattern. (f) Binary dithered image of (e) using Bayer-ordered dithering technique. (g) Binary dithered image of (e) with the Floyd–Steinberg error-diffusion technique. (h) Binary dithered image of (e) with the Stucki error-diffusion technique.

dithering has succeeded in providing valid results in 3D shape measurement [32].

Error-diffusion techniques are more extensively employed since they can better represent the original image with the quantization errors being propagated. For each error-diffusion technique, the pixels are quantized in a specific order such that the quantization error of the pixel in process is propagated forward to the local unprocessed pixels. Its basic principle can be described by the following equation:

$$\tilde{f}(i,j) = f(i,j) + \sum_{k,l \in S} h(k,l)e(i-k,j-l) \quad (9)$$

Here, $f(i,j)$ refers to the pixel of the original image, $\tilde{f}(i,j)$ stands for the modified input pixel. The modified input pixel $\tilde{f}(i,j)$ is then quantized and the output image is obtained. This equation explains how the quantization error $e(i,j)$ is propagated to the neighboring pixels by applying a 2-D weighted function $h(i,j)$, which is known as diffusion kernel. There are a variety of error-diffusion algorithms developed based on different selected diffusion kernels. Floyd–Steinberg error-diffusion and Stucki error-diffusion techniques are the two most extensively used error-diffusion techniques. The diffusion kernel of Floyd error-diffusion algorithm is written as

$$h(i,j) = \frac{1}{16} \begin{bmatrix} - & * & 7 \\ 3 & 5 & 1 \end{bmatrix}, \quad (10)$$

Here, $-$ refers to the previously processed pixel, $*$ represents the pixel in process. It is worth to note that the kernel elements should sum to one so that the local average of the image does not change. Similarly, Stucki error-diffusion kernel is written as

$$h(i,j) = \frac{1}{42} \begin{bmatrix} - & - & * & 8 & 4 \\ 2 & 4 & 8 & 4 & 2 \\ 1 & 2 & 4 & 2 & 1 \end{bmatrix}, \quad (11)$$

2.6. Optimized-dithering techniques

Since dithering techniques are simply applying a matrix to the image, it is far from optimal. Also, the improvement could be rather limited when the fringe stripes are narrow. Then further attempts are made to improve dithering techniques, which include the phase optimization algorithm proposed by Dai and Zhang [35], and the genetic algorithm proposed by Lohry and Zhang [34].

Phase optimization algorithm, designed to improve the dithering technique, has succeeded in reducing its overall phase error. The major framework of this proposed method can be described by the following steps: First, the error pixels need to be detected. Here, an error pixel refers to the pixel that has phase error above a certain threshold. Specifically, the three-step phase-shifting algorithm is used to extract the phase both from ideal sinusoidal pattern and from the dithered pattern after Gaussian smoothing, and the phase error is then computed by taking the difference between these two phase maps. Second, the detected error pixels are mutated (i.e. 1–0 s or 0–1 s). The mutation is kept if the phase error becomes smaller or withdrawn otherwise. Third, this whole algorithm needs to be performed iteratively since if one of the pixels is altered, its neighboring pixels would also be affected after Gaussian smoothing. Therefore, after getting the whole pattern, it would go back to the previous step until the phase error converges. Finally, the threshold is reduced to a smaller number and the whole algorithm goes back to the first step. Here, for all fringe periods that we tested with this algorithm, we found that the phase errors become sufficiently small after 15 iterations, and thus the algorithm terminates after 15 iterations for all cases. Fig. 6 (b) shows an example pattern resulted from the phase optimization algorithm when the fringe period is $T=18$ pixels.

Genetic algorithm, despite of its being a time-consuming method, has been proved successful in improving the error-diffusion techniques especially when the fringe stripes are narrow. To start with, notably, the error-diffusion technique is path and origin dependent, and thus different genes can be generated with different starting point. The optimization process could be sped up

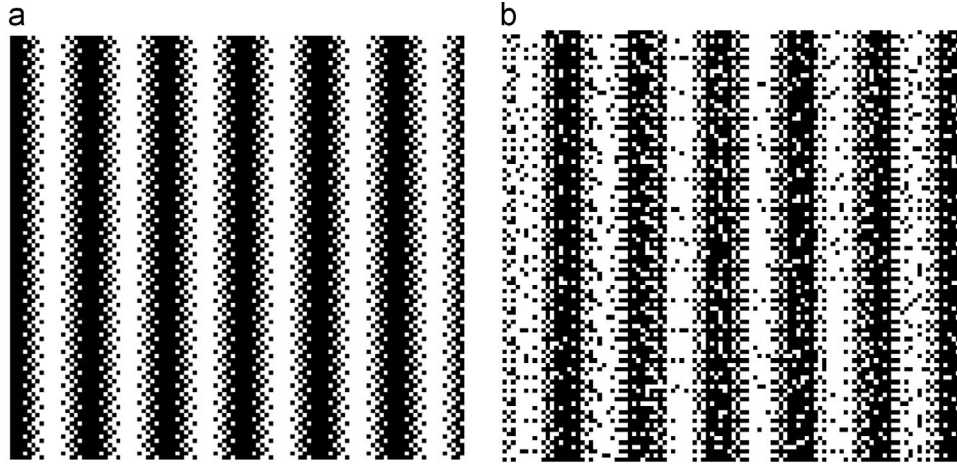


Fig. 6. (a) An example pattern of genetic algorithm with $T=18$. (b) An example pattern of phase optimization algorithm with $T=18$.

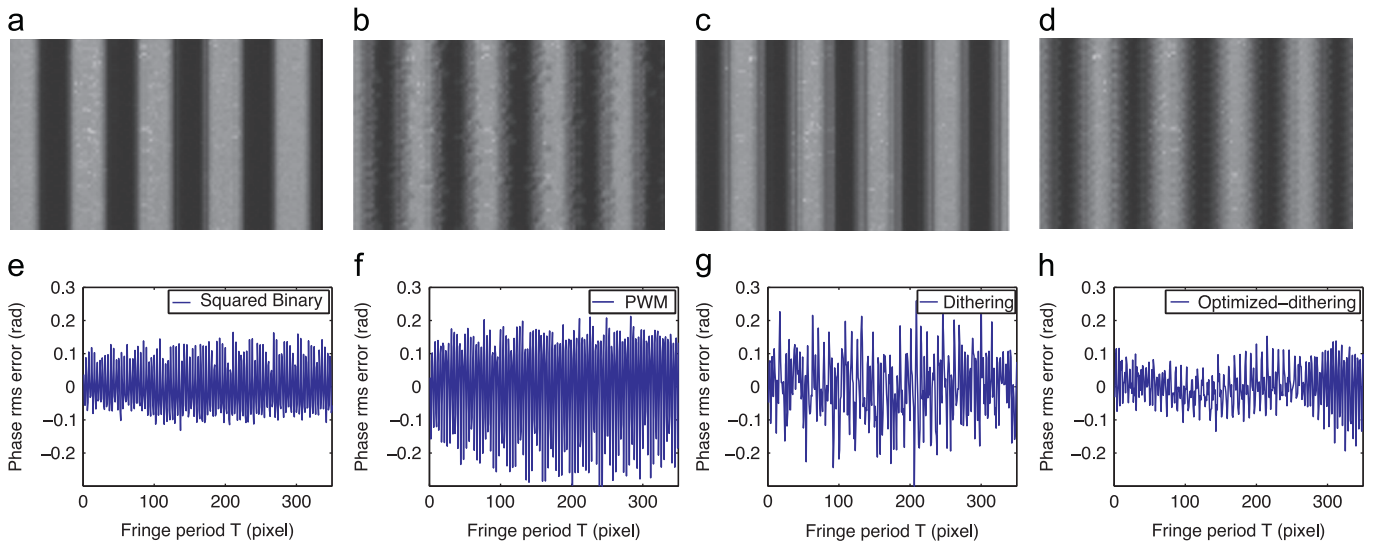


Fig. 7. Captured patterns with the fringe period $T=18$ pixels when the projector is nearly focused (a) squared binary pattern; (b) PWM pattern; (c) dithering pattern; (d) optimized-dithering pattern; and (e and f) corresponding error cross-section plots of (a–d) with standard phase rms errors of 0.08 rad, 0.15 rad, 0.10 rad and 0.06 rad, respectively.

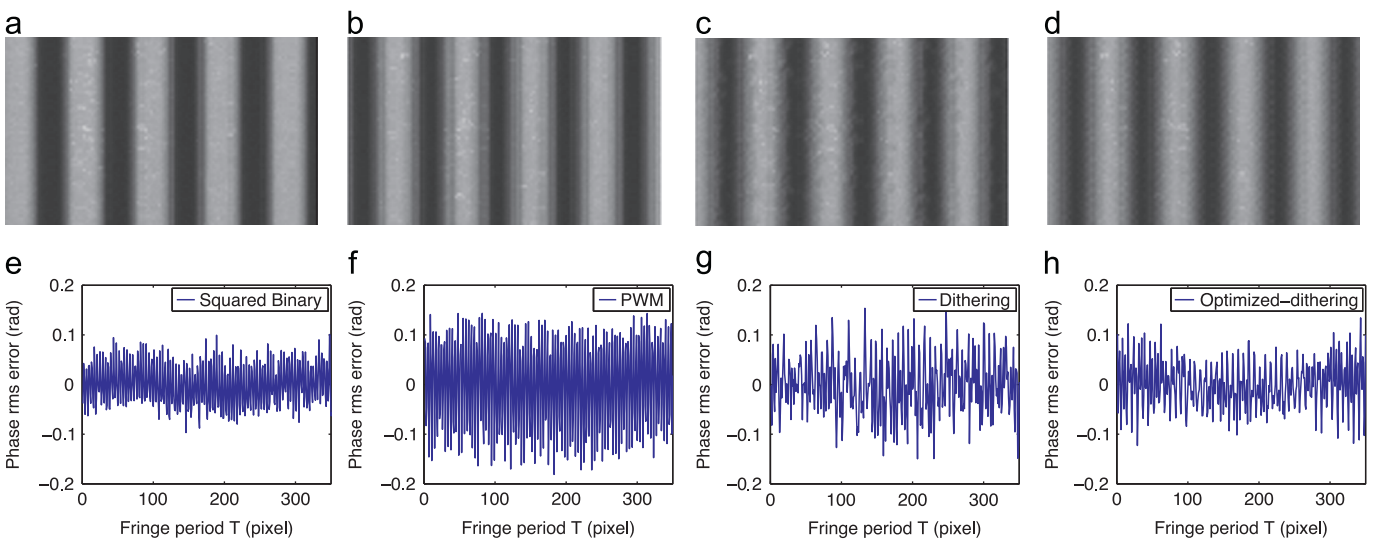


Fig. 8. Captured patterns with the fringe period $T=18$ when the projector is more defocused (a) squared binary pattern; (b) PWM pattern; (c) dithering pattern; (d) optimized-dithering pattern; and (e and f) corresponding error cross-section plots of (a–d) with standard phase rms errors of 0.048 rad, 0.092 rad, 0.059 rad and 0.054 rad, respectively.

with the diversity of variations. Within this proposed algorithm, two major techniques are used: crossover and mutation. Crossover means to copy a block of one pattern to another one, this could happen when two patterns are selected for recombination. Mutation is a technique that flips the bits (i.e. 1–0 s or 0–1 s) within the regions detected with larger errors. These two methods (mutation

and crossover) can be applied in different ways to create a population of 20 individuals in each generation. A fitness function, which is defined as the difference between the designed patterns after Gaussian smoothing with the ideal sinusoidal pattern, is used to evaluate individuals within each generation. Then, a rank selection method is served as a criterion for choosing the best

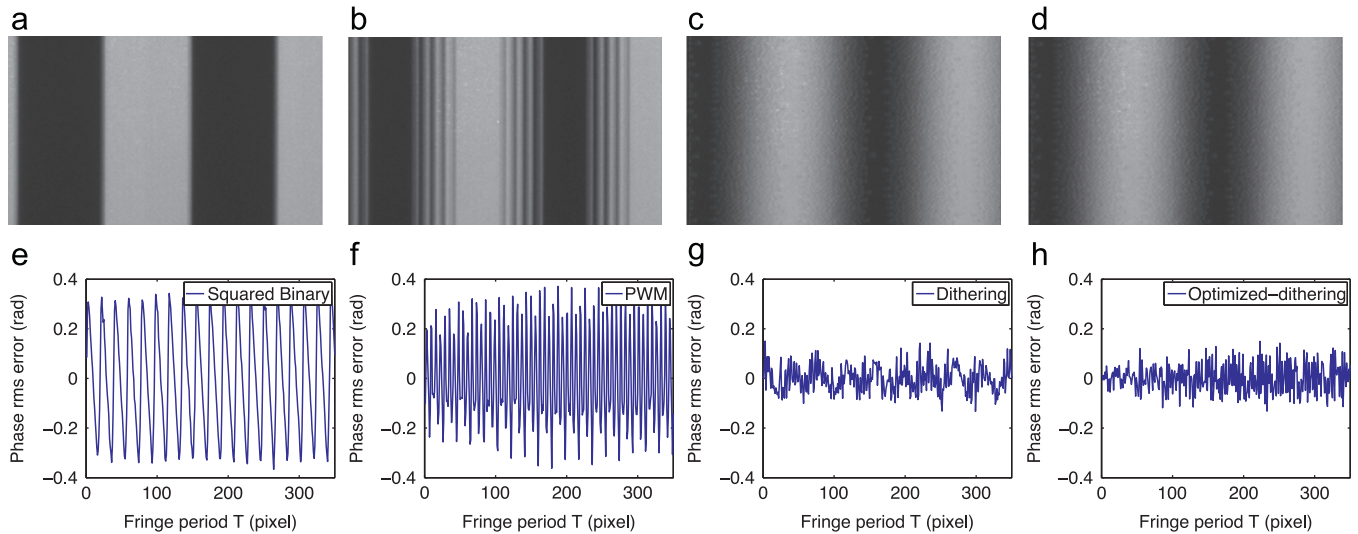


Fig. 9. Captured patterns with the fringe period $T=90$ pixels when the projector is nearly focused. (a) squared binary pattern; (b) PWM pattern; (c) dithering pattern; (d) optimized-dithering pattern; and (e and f) corresponding error cross-section plots of (a–d) with standard phase rms errors of 0.2176 rad, 0.1846 rad, 0.0534 rad and 0.0525 rad, respectively.

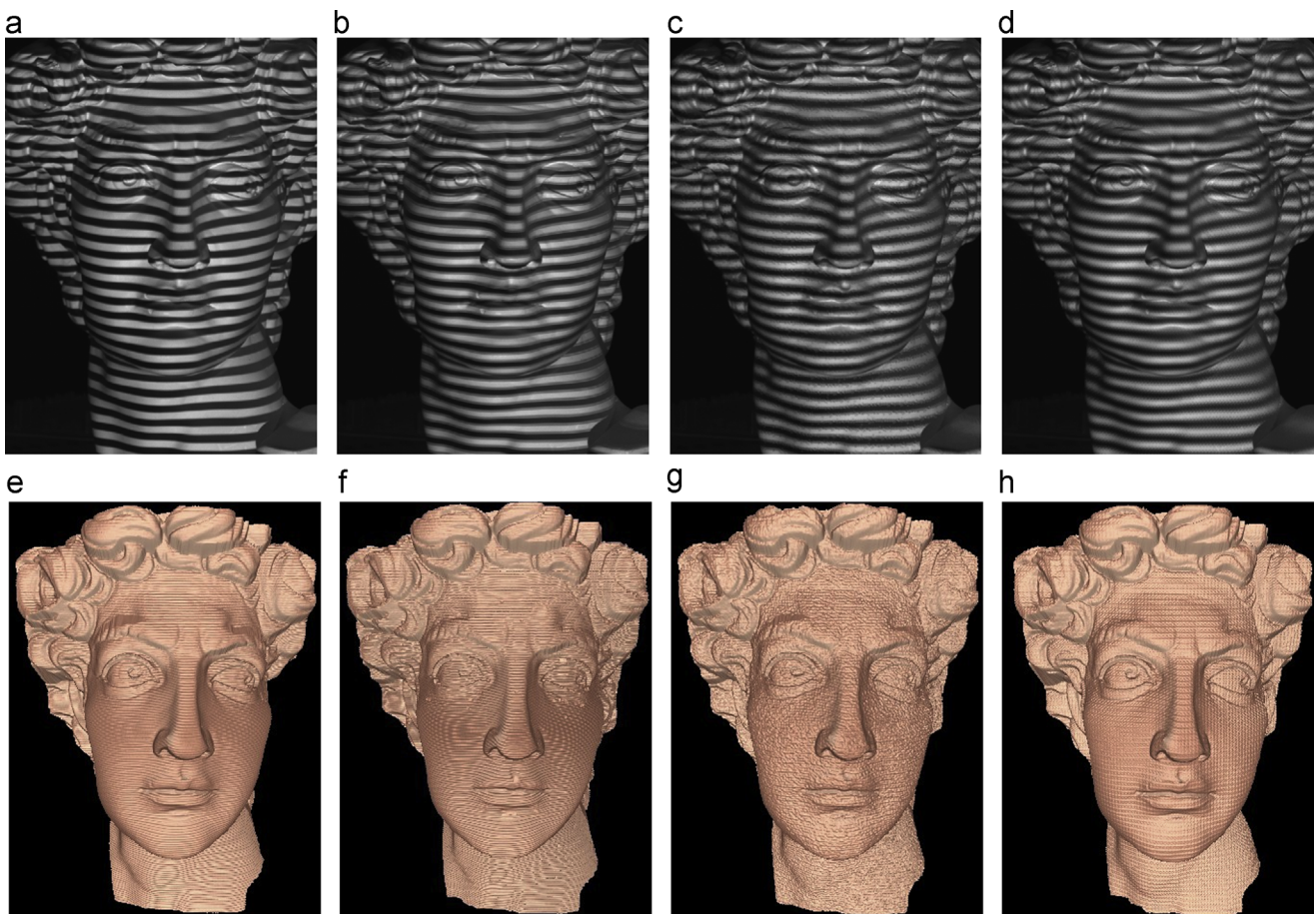


Fig. 10. Captured patterns with the fringe period $T=18$ when the projector is nearly focused (a) squared binary pattern; (b) PWM pattern; (c) dithering pattern; (d) optimized-dithering pattern; and (e and f) corresponding reconstructed 3D results of (a–d);

individuals as the parents for the next generation. By varying crossover and mutation, the whole process could be sped up and optimized [34]. Fig. 6(a) shows an example pattern generated by the genetic algorithm when the fringe period is $T=18$.

We have demonstrated that, overall, both algorithms could substantially improve the fringe quality with the genetic algorithm out-performing the phase-optimized method, even though the genetic algorithm takes much longer to converge, and sometimes cannot generate the optimal results.

3. Experimental results

Experiments were performed in order to examine the performances of the proposed techniques. A 3D shape measurement system was developed which includes a digital-light-processing (DLP) projector (Samsung SP-P310MEMX) and a charge-coupled-device (CCD) camera (Jai Pulnix TM-6740CL). The camera is attached with a 16 mm focal length Mega-pixel lens (Computar M1614-MP) with F/1.4 to 16C. The camera has a resolution of 640×480 , and the projector has a native resolution of 800×600 with a projection distance of 0.49–2.80 m.

To start with, a flat white board was first measured using the squared binary patterns, the pulse width modulation (PWM) patterns, the dithered patterns, and the optimized-dithering patterns. Here, the OPWM, the Stucki error-diffusion, and the genetic algorithm are chosen to respectively represent the PWM techniques, the dithering techniques, and the optimized-dithering techniques. The flat board was first measured with the fringe

period of $T=18$ pixels and nearly focused. Fig. 7 shows the experiment results when the projector is nearly focused, from which it is discovered that optimized-dithering technique has the best performance, while PWM technique and dithering technique fail to provide better results than SBM. Here, as well the following experiments, the phase error was computed by taking the difference between the phase obtained from these pattern with the phase obtained by a nine-step phase-shifting algorithm with a fringe period of $T=18$ pixels.

We then measured the same board when the projector was further defocused. Similarly, the experiment was also carried out using the same fringe period ($T=18$ pixels). Fig. 8 shows the results. This experiment indicates that the SBM has the least phase error, which means that if the projector is defocused more, none of the optimization techniques could outperform the natural SBM. This is because when the fringe period is very small, the natural defocusing can successfully suppress all high-order harmonics, and any changes to the original squared pattern will deteriorate the suppression performance.

We also measured the flat board using a larger fringe period ($T=90$ pixels). Fig. 9 shows the results when the projector is nearly focused. This experiment clearly shows that neither the SBM nor the PWM technique could provide reasonable result, despite the little improvement that the PWM technique has over the SBM. Dithering technique and optimized-dithering technique could generate good phase, with the optimized dithering technique being slightly better than the Stucki-dithering technique.

Furthermore, a more complex 3D sculpture was measured to visually compare these techniques. Fig. 10 illustrates the reconstructed

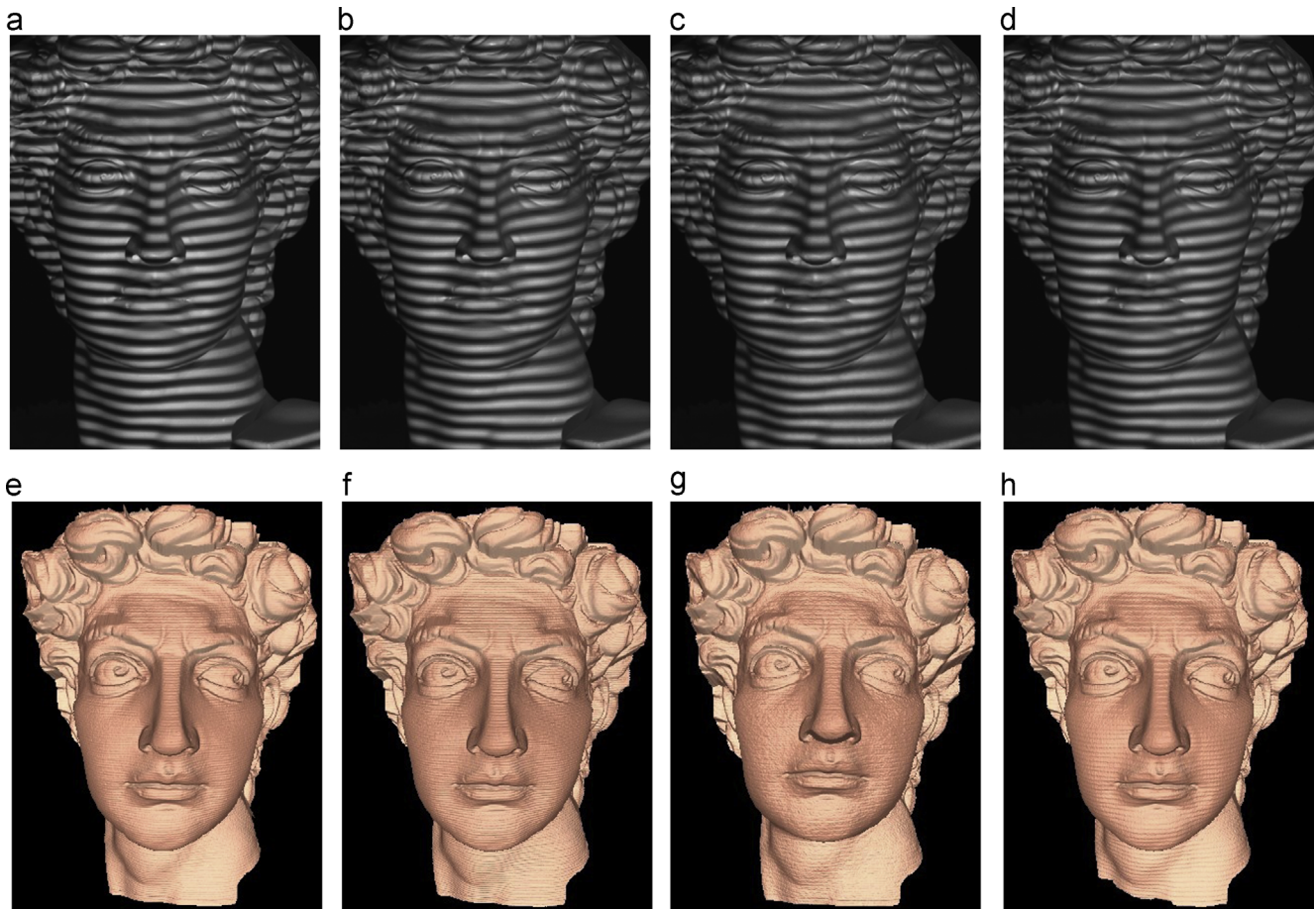


Fig. 11. Captured patterns with the fringe period $T=18$ pixels when the projector is more defocused. (a) Squared binary pattern; (b) PWM pattern; (c) dithering pattern; (d) optimized-dithering pattern; and (e and f) corresponding reconstructed 3D results of (a–d).

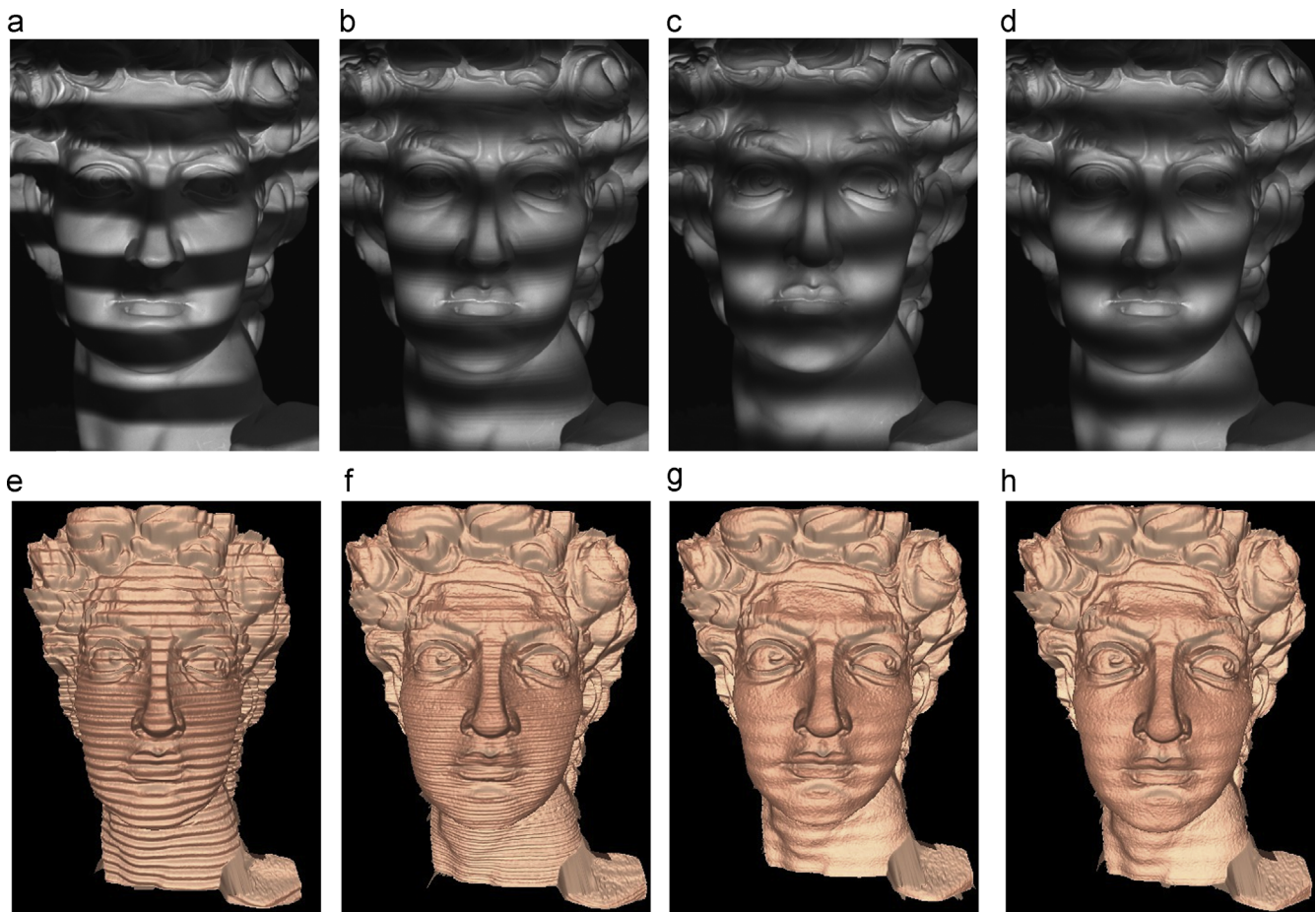


Fig. 12. Captured patterns with the fringe period $T=90$ pixels when the projector is slightly defocused. (a) Squared binary pattern; (b) PWM pattern; (c) dithering pattern; (d) optimized-dithering pattern; and (e and f) Corresponding reconstructed 3D results of (a–d).

3D results when the fringe period $T=18$ pixels was used with the projector being nearly focused, from which it can be clearly seen that PWM technique and dithering technique cannot generate phase with good quality, while optimized-dithering shows little improvement over the SBM technique, although the difference between the two is relatively small. In this research, we adopted the computational framework described in Ref. [36] to unwrap the phase, and the reference-plane based method to convert phase to depth. The details of the reference-plane based method was discussed in Ref. [13].

We then further defocused the projector and performed the measurement again. Fig. 11 shows the results using the same fringe period. This experiment indicates that, again, none of the optimization techniques can outperform the SBM technique. In other words, the SBM is already good enough if narrow fringe stripes are used and the projector is slightly defocused.

The 3D sculpture was also measured under the fringe period $T=90$ pixels with the projector being slightly defocused (at the same level as experiment presented in Fig. 11). Fig. 12 shows the results. This experiment shows that neither the SBM nor the PWM can generate high-quality 3D results, despite the small enhancement that PWM has on SBM. While dithering technique and optimized-dithering technique could perform well in reconstructing the phase of the sculpture, and also, there is quite a clear improvement that optimized-dithering has upon dithering technique. This experiment indicates that when fringe stripes are wide, either dithering technique or the optimized dithering technique shall be adopted for high-quality 3D shape measurement.

Finally, we developed a system to measure live rabbit hearts that beats at approximately 200 beats per minutes [33]. The

system is composed of a digital-light-processing (DLP) projector (DLP LightCrafter, Texas Instruments, TX), a high-speed CMOS camera (Phantom V9.1, Vision Research, NJ). The camera was triggered by an external electronic circuit that senses timing signal of the DLP projector. The camera was set to capture images with a resolution of 576×576 , and the projector has a resolution 608×648 . The projector was set to switch binary patterns at 2000 Hz, and the camera was chosen to capture at 2000 Hz. Two wavelength phase-shifting technique was chosen with the shorter wavelength being OPWM pattern and longer wavelength being Stucki-dithered patterns.

Fig. 13 shows some typical results of a rabbit heart. It clearly shows that the dynamic motion of the heart was well captured. Without the binary defocusing techniques, the live heart rabbit surface could not be properly measured as we found that at least 800 Hz was required to properly measure the heart without obvious motion artifacts.

4. Conclusions

This paper summarized the binary defocusing techniques originally developed to achieve superfast 3D shape measurement, and to overcome the problems associated with conventional digital fringe projection techniques. Advances have been made to permit the binary defocusing technique using nearly focused projector to achieve high-quality 3D shape measurement. Our experiments also found that when the fringe stripes are narrow, and the projector is slightly defocused, the conventional squared

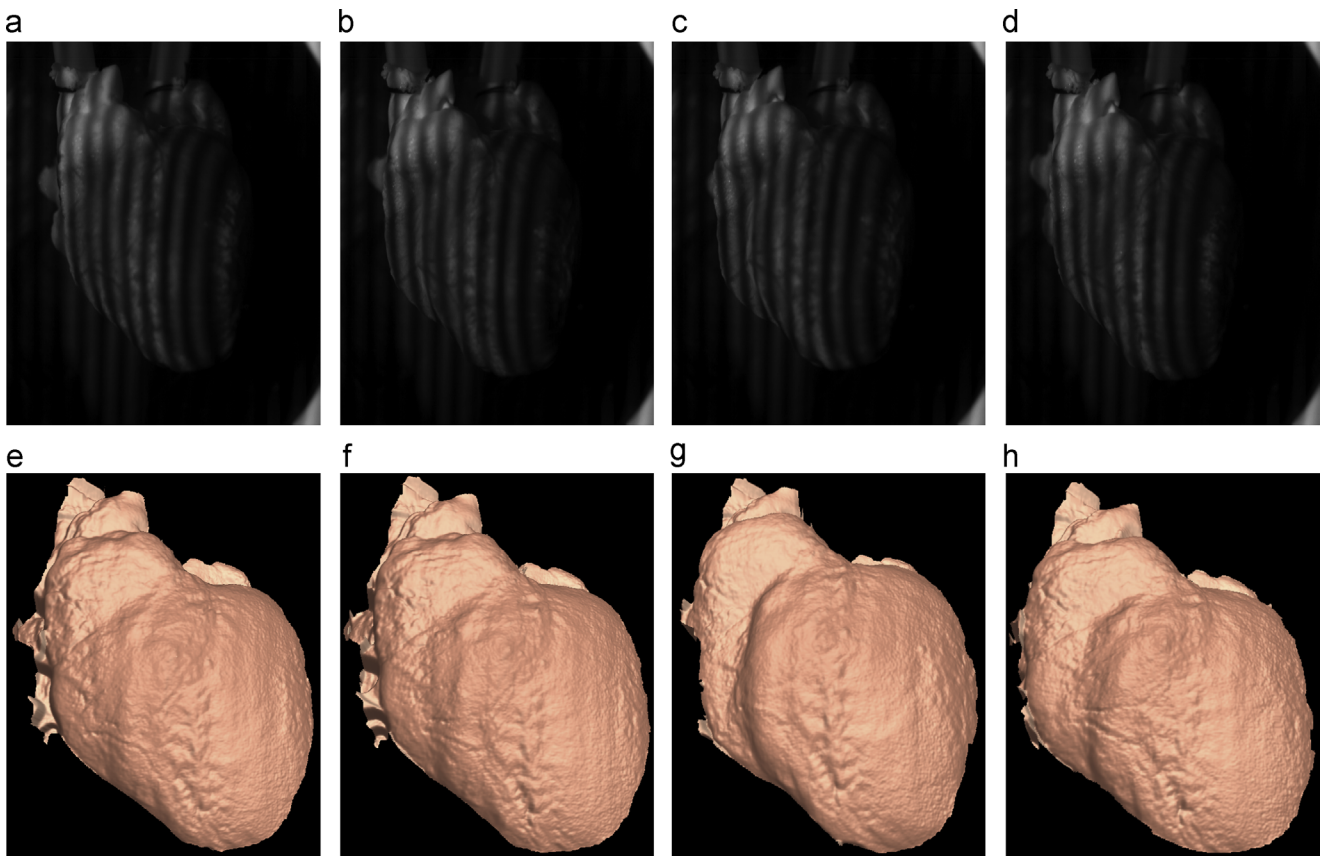


Fig. 13. Example of capturing live rabbit hearts with binary defocusing techniques. (a–d) Captured fringes of a live rabbit heart; and (e and f) corresponding reconstructed 3D results of (a–d).

binary patterns provides the best results; when the fringe stripes are wide, the dithering techniques could drastically improve measurement quality. The optimized dithering techniques could further improve the measurement quality when the projector is nearly focused, yet, their improvement was not significant when fringe stripes are narrow. We believe that there is still large room to further improve the dithering technique to achieve superior quality 3D shape measurements as long as the projector is not perfectly focused. Future efforts will be focused on developing method to generate optimal binary patterns for 3D shape measurement.

Acknowledgments

The authors would like to thank graduate student Jacob I. Laughner and Professor Igor R. Efimov from Washington University in St. Louis for their help on the heart measurements. All heart data were captured in Prof. Efimov's lab with the assistance of Mr. Laughner. The authors would also like to thank the National Science Foundation (NSF) to sponsor this project. The NSF grant numbers are CMMI-1150711 managed by program officer Dr. George Hazelrigg and CMMI-1300376 managed by program officer Dr. Zhijian Pei.

References

- [1] Geng J. Structured-light 3D surface imaging: a tutorial. *Adv Opt Photon* 2011;3(2):128–60.
- [2] Gorthi S, Rastogi P. Fringe projection techniques: Whither we are?. *Opt Laser Eng* 2010;48:133–40.
- [3] Zhang S. Recent progresses on real-time 3-D shape measurement using digital fringe projection techniques. *Opt Laser Eng* 2010;48(2):149–58.
- [4] Lei S, Zhang S. Digital sinusoidal fringe generation: defocusing binary patterns vs focusing sinusoidal patterns. *Opt Laser Eng* 2010;48(5):561–9.
- [5] Kakunai S, Sakamoto T, Iwata K. Profile measurement taken with liquid-crystal grating. *Appl Opt* 1999;38(13):2824–8.
- [6] Guo H, He H, Chen M. Gamma correction for digital fringe projection profilometry. *Appl Opt* 2004;43:2906–14.
- [7] Pan B, Kemao Q, Huang L, Asundi A. Phase error analysis and compensation for nonsinusoidal waveforms in phase-shifting digital fringe projection profilometry. *Opt Lett* 2009;34(4):2906–14.
- [8] Huang PS, Zhang C, Chiang F-P. High-speed 3-D shape measurement based on digital fringe projection. *Opt Eng* 2002;42(1):163–8.
- [9] Zhang S, Huang PS. Phase error compensation for a three-dimensional shape measurement system based on the phase shifting method. *Opt Eng* 2007;46(6):603–601.
- [10] Zhang S, Yau S-T. Generic nonsinusoidal phase error correction for three-dimensional shape measurement using a digital video projector. *Appl Opt* 2007;46(1):36–43.
- [11] Lei S, Zhang S. Flexible 3-D shape measurement using projector defocusing. *Opt Lett* 2009;34(20):3080–2.
- [12] Zhang S, van der Weide D, Oliver J. Superfast phase-shifting method for 3-D shape measurement. *Opt Express* 2010;18(9):9684–9.
- [13] Xu Y, Ekstrand L, Dai J, Zhang S. Phase error compensation for three-dimensional shape measurement with projector defocusing. *Appl Opt* 2011;50(17):2572–81.
- [14] Merner L, Wang Y, Zhang S. Accurate calibration for 3D shape measurement system using a binary defocusing technique. *Opt Laser Eng* 2013;51(5):514–9.
- [15] Wang Y, Zhang S. Superfast multifrequency phase-shifting technique with optimal pulse width modulation. *Opt Express* 2011;19(6):5143–8.
- [16] Ekstrand L, Zhang S. Three-dimensional profilometry with nearly focused binary phase-shifting algorithms. *Opt Lett* 2011;35(23):4518–20.
- [17] Zhang S, Wang Y, Laughner JI, Efimov IR. Measuring dynamic 3D microstructures using a superfast digital binary phase-shifting technique. In: *ASME 2013 international manufacturing science and engineering conference*, Madison, Wisconsin; 2013.
- [18] Fujita H, Yamatan K, Yamamoto M, Otani Y, Suguro A, Morokawa S, et al. Three-dimensional profilometry using liquid crystal grating. In: *Proceedings of the SPIE*, vol. 5058. Beijing, China; 2003. p. 51–60.
- [19] Yoshizawa T, Fujita H. Liquid crystal grating for profilometry using structured light. In: *Proceedings of the SPIE*, vol. 6000. Boston, MA; 2005. 60,000H1–10.
- [20] Ayubi GA, Ayubi JA, Martino JMD, Ferrari JA. Pulse-width modulation in defocused 3-D fringe projection. *Opt Lett* 2010;35:3682–4.

- [21] Wang Y, Zhang S. Optimum pulse width modulation for sinusoidal fringe generation with projector defocusing. *Opt Lett* 2010;35(24):4121–3.
- [22] Zuo C, Chen Q, Feng S, Feng F, Gu G, Sui X. Optimized pulse width modulation pattern strategy for three-dimensional profilometry with projector defocusing. *Appl Opt* 2012;15(19):4477–90.
- [23] Wang Y, Zhang S. Comparison among square binary, sinusoidal pulse width modulation, optimal pulse width modulation methods for three-dimensional shape measurement. *Appl Opt* 2012;51(7):861–72.
- [24] Xian T, Su X. Area modulation grating for sinusoidal structure illumination on phase-measuring profilometry. *Appl Opt* 2001;40(8):1201–6.
- [25] Lohry W, Zhang S. 3D shape measurement with 2D area modulated binary patterns. *Opt Laser Eng* 2012;50(7):917–21.
- [26] Schuchman TL. Dither signals and their effect on quantization noise. *IEEE Trans. Commun. Technol.* 1964;12(4):162–5.
- [27] Purgathofer W, Tobler R, Geiler M. Forced random dithering: improved threshold matrices for ordered dithering. In: *IEEE international conference on image processing*, vol. 2; 1994. p. 1032–35.
- [28] Bayer B. An optimum method for two-level rendition of continuous-tone pictures. In: *IEEE international conference on communications*, vol. 1; 1973. p. 11–15.
- [29] Kite TD, Evans BL, Bovik AC. Modeling and quality assessment of Halftoning by error diffusion. In: *IEEE international conference on image processing*, vol. 9 (5); 2000. p. 909–22.
- [30] Floyd R, Steinberg L. An adaptive algorithm for spatial gray scale. In: *Proceedings of the society for information display*, vol. 17(2); 1976. p. 75–77.
- [31] Stucki P. MECCA: a multiple-error correcting computation algorithm for bilevel hardcopy reproduction. Technical Report, IBM Res. Lab., Zurich, Switzerland; 1981.
- [32] Wang Y, Zhang S. Three-dimensional shape measurement with binary dithered patterns. *Appl Opt* 2012;51(27):6631–6.
- [33] Wang Y, Laughner JI, Efimov IR, Zhang S. 3D absolute shape measurement of live rabbit hearts with a superfast two-frequency phase-shifting technique. *Opt Express* 2013;21(5):5632–822.
- [34] Lohry W, Zhang S. Genetic method to optimize binary dithering technique for high-quality fringe generation. *Opt Lett* 2013;38(4):540–2.
- [35] Dai J, Zhang S. Phase-optimized dithering technique for high-quality 3D shape measurement. *Opt Laser Eng* 2013;51(6):790–5.
- [36] Zhang S. Flexible 3-D shape measurement using projector defocusing: extended measurement range. *Opt Lett* 2010;35(7):931–3.